

Distress Due to Sun Camber in a Long-Span Roof of a Parking Garage

by Mark Fintel and S. K. Ghosh

Distress in a 9-story cast-in-place concrete parking garage is described. A detailed account is given of field observations, measurements, and computations leading to a definite diagnosis for the distress. A repair procedure that accommodates unavoidable movements of the structure is outlined.

The vertical deflections due to direct solar radiation acting on the roof of a 60-ft (18.3-m) span post-tensioned parking garage caused severe diagonal cracking of the supporting beams and horizontal cracks in the supporting columns.

A program of field measurement of slab temperatures and deflections was carried out during the Summer of 1984. Twenty sets of measurements were compiled. The plots of average slab temperatures, sun camber, and crack width in supporting columns were almost identical in shape. The measured slab deflections were close to those predicted analytically.

The structure

The 9-story cast-in-place parking garage in Birmingham, Alabama has three 60 ft (18.3 m) bays in the east-west direction. The east and west bays (Fig. 1) slope up and down respectively, a half story height in a 200 ft (61 m) length. The structure is 363 ft (110.6 m) long in the N-S direction. Columns in that longitudinal direc-

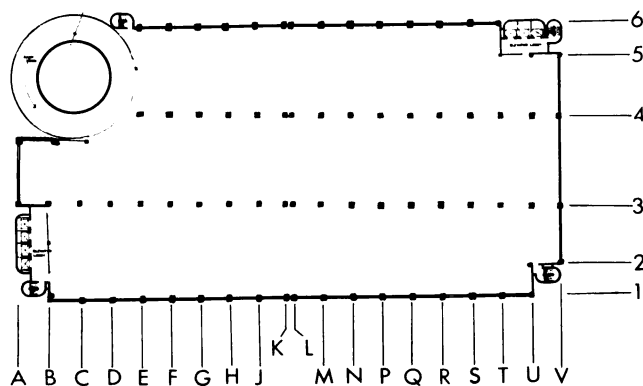


Fig. 1 — Typical floor plan of garage

tion are spaced at 20 ft (6.1 m) on centers. An expansion joint (with double columns) divides the garage into two halves.

The 60 ft (18.3 m) spans have 18 x 24 in. (457 x 610 mm) post-tensioned beams on 5 ft (1.5 m) centers. The slab between the post-tensioned beams is a nominally post-tensioned 4 in. (102 mm) plate. The beams supporting the 60 ft (18.3 m) span slab system are post-tensioned over their 20 ft (6.1 m) spans and are of the same 24 in. (610 mm) depth as the slab beams.

The exterior support beams are 46 in. (1168 mm) wide, the interior split beams of the sloped bays are 18 in. (457 mm) wide. The interior columns are 28 x 28 in. (711 x 711 mm); the exterior columns are 24 x 30 in. (610 x 762 mm) with rounded exterior corners. There is a double helix speed exit ramp on the north-east corner of the building.

Construction of the structure started in the summer of 1974 and was completed in the spring of 1976.

Cracking history

Cracks in the sloped split beams of the top floor on column lines 3 and 4 (Fig. 1) were initially reported in October of 1977. Over the years (up to 1984) these cracks were repeatedly repaired with various patching materials. In most cases the patches either cracked or spalled off and the cracks reappeared.

An inspection in April, 1984 revealed two separate areas of distress:

- The interior beams and exterior columns supporting the roof ramps.
- The exterior beams supporting the ramp down from the first level of the west bay.

Interior beams and exterior columns at roof level

The 18 x 24 in. (457 x 610 mm) interior (split) supporting beams of the sloped east and west bays of the uppermost level showed cracks generally on all four faces, (Fig. 2). These split beams on column lines 3 and 4 extend over 10 bays between lines F and S. The diagonal cracking at the beam ends ranged from slight to

Keywords: camber; cracking (fracturing); measurement; parking structures; repairs; solar radiation; thermal gradient; thermal stresses.

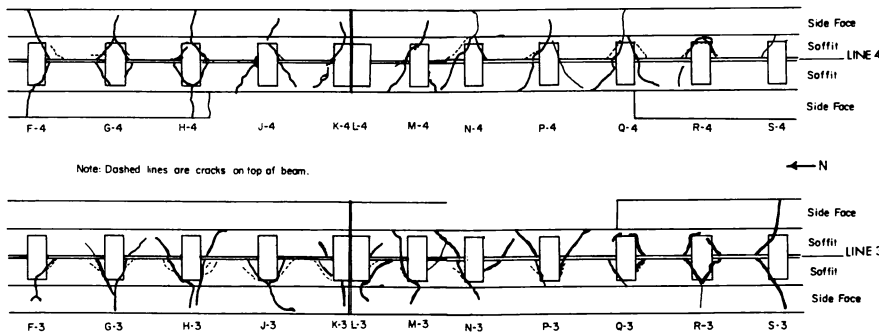


Fig. 2 — Cracks on faces of sloped split beams on lines 3 and 4 of level 8-9 (not to scale).

severe (Figs. 3 and 4). The diagonal cracks were patched over the years with different materials (apparently in different operations at various times). The repairs did not prevent repeated cracking, although some of the patching material seemed quite flexible.

The inclined beams frame into the 28 x 28 in. (711 x 711 mm) interior columns on lines 3 and 4 at various levels within their story heights. These same columns receive on their other halves (facing the middle bay) split beams of the 8th and 9th level horizontal middle bays at their bottoms and tops, respectively (Fig. 5).

Some column corners under the inclined beams had spalled off, or the patch material separated, usually following the direction of previous cracks at the beam soffit. The nature of the cracks indicated that an upward motion of the slab bay and pull of the slabs created tensile forces that separated the patches from the column corners.

At the uppermost horizontal central bay, a line of separation (Fig. 5) at the interior interface between beams and columns was observed in many cases, with no distress, however, in the beams. This indicated that the absence of a strong restraint (no column above) allowed these beams to rotate without suffering torsional cracks. At the corresponding exterior (east and west) ends of the sloped bays, there were horizontal cracks observed on the interior faces of the exterior columns about 15 to 20 in. (381 to 508 mm) under the beams. The depth of the cracks reached only about 1/4 of the

column depth (Fig. 5). Three of these cracks measured 5, 6, and 10 thousandths of an inch (0.127, 0.152 and 0.254 mm) wide in the late afternoon of April 12 (air temperature 75F [23.9C]) and half as wide the next morning (air temperature 60 F [15.6 C]).

Measurements with an ordinary level instrument of midspan slab elevations over the 60 ft (18.3 m) span of the sloped roof (east bay) in the morning and afternoon showed an upward deflection (sun camber) of 0.194 in. (4.9 mm) for an air temperature increase of 13°F (7.2°C) on a partly cloudy day.

Assumed reasons for cracking

The following items were considered in determining reasons for cracking of the sloped beams supporting the 60-ft (18.3-m) span east and west roof bays:

- The beams cracked and re-cracked after repeated repairs, indicating either a continuation of creep movement due to post-tensioning, or a cyclic movement of the 60-ft (18.3-m) span slabs due to seasonal or daily temperature changes.
- The possibility that creep and shrinkage across the 3-bay structure might have caused distress at the roof level only was disregarded, since the entire structure shrinks and creeps, without creating distortions from story to story. Only between the ground level and the first framed floor are there creep and shrinkage differentials to be considered.
- The supporting beams on all floors are subject to



Fig. 3 — Cracks at column H4.



Fig. 4 — Cracks at column G4.

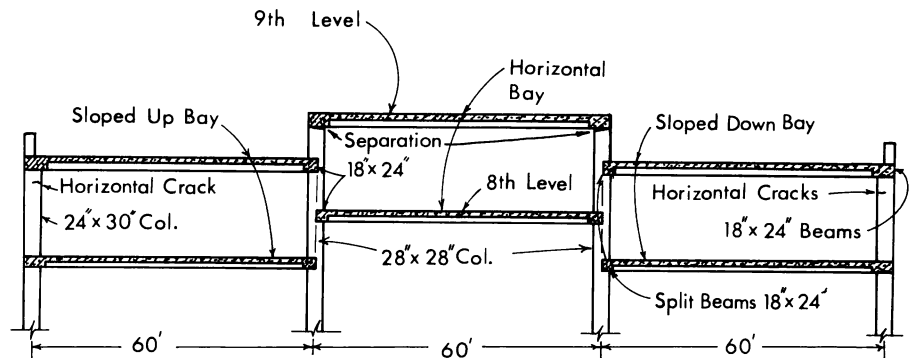


Fig. 5 — Transverse section at top of structure (not to scale)

vertical shear due to dead and live loads on the slabs, and horizontal shear due to post-tensioning of the slab beams and subsequent creep. The absence of cracking of the supporting beams on all floors (except roof) indicates sufficient capacity to resist these forces.

- The cracks shown in Fig. 2 on the tops and on the soffits of the inclined beams are in the same direction, indicating that horizontal forces due to post-tensioning and creep from post-tensioning pull on the beams horizontally toward the slab span.
- The direct solar radiation on all three roof bays causes a thermal gradient in the 4-in. (102-mm) thick slabs and in the slab beams, which results in an upward deflection (sun camber) of the 60 ft (18.3 m) span, and a consequent rotation of supports.
- The supporting beams of the sloped side bay roofs (on lines 3 and 4) are restrained against rotation and against horizontal shortening by short, rigid columns below and above (Fig. 5).
- The supporting beams of the horizontal middle bay roof have some rotational freedom since they are restrained against rotation only by the columns below (Fig. 5).

As consequences of the items discussed above:

- The slab beams of the horizontal middle bay roof, having less rotational restraint, could rotate upward at the supports and cause a cracked separation at the interface between columns and beams (Fig. 5). Also, the absence of columns above permitted some inward movement of the column tops caused by elastic and creep shortening of the post-tensioned slabs; thus the beams did not crack diagonally.

- The interior beams of the sloped side bay roofs, restrained against rotation above and below by the relatively large 28 x 28 in. (711 x 711 mm) short columns (say half story high), cracked because of the addition of torsional stresses caused by upward thermal slab deflections to the previously high vertical and horizontal shear stresses.
- The relatively large exterior beams of the sloped roof bays were not restrained by columns above. They rotated together with the long-span slab bowed up by the sun, and induced horizontal cracks on the inside face of the columns about 15 in. (381 mm) under the beams (Fig. 5).

Field observations and sun camber computations

To test the validity of the assumed reasons for the observed distress, a field investigation was carried out during the summer of 1984 to determine the effects of summer temperatures and direct solar radiation on the structure, and to establish a definite correlation between temperature variations and structural performance. Sun camber computations were carried out for comparison with the measured upward deflections of the garage roof.

Between May 1, 1984 and November 2, 1984, twenty of the following observations and measurements were made, to compile the necessary data:

- Temperatures of the top and bottom of the 4-in. (102-mm) thick slab and the underside of the slab joists (Fig. 6), using a surface thermometer.

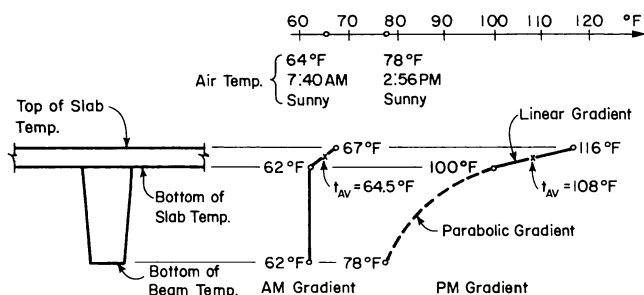


Fig. 6 — Sample of measured temperatures.

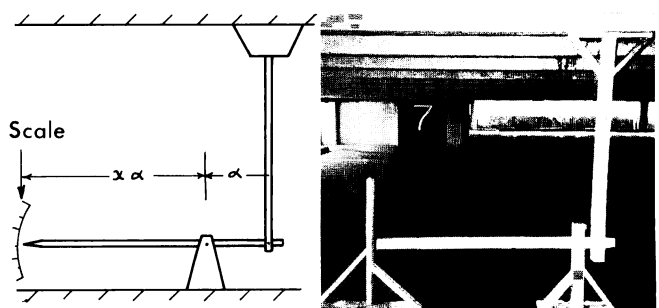


Fig. 7 — Deflection measuring device.

Table 1 — Summary of recorded data

Date 1984	Time AM-PM	Air temp. (F)	Air temp. diff. (F)	Sky	Temperatures (F)					Slab lvl. (in.)	Slab lvl. diff. (in.)	Sun camber (in.)*	Col. crack width ($\frac{\text{in.}}{1000}$)	Diff.
					Slab top	Slab bott.	Beam bott.	Ave	Diff. AM-PM					
(1)	(2)	(3)	(4)	(5)	(6)	(7)	(8)	(9)	(10)	(11)	(12)	(13)	(14)	(15)
5/01	7:40A 2:45P	59 72	13	Sunny Ovrcest	64 74	— —	— —	— —	— —	1.85 4.05	2.20	0.194	0.67 3.00	2.23
5/07	10:00A 3:05P	79 86	7	Prt.Cl Prt.Cl	91 110	— —	— —	— —	— —	2.30 4.80	2.50	0.220	2.00 5.25	3.25
5/10	8:33A 3:10P	63 76	13	Sunny Sunny	73 109	— —	— —	— —	— —	2.63 8.25	5.62	0.496	0.50 7.50	7.00
5/17	7:40A 2:45P	61 78	17	Sunny Sunny	64 110	63 104	61 90	63.0 104.0	41.0	2.19 8.38	6.19	0.546	0.50 9.25	8.75
5/23	7:34A 3:52P	72 81	9	Sunny Ovrcest	80 91	72 90	72 81	74.3 89.4	15.1	2.00 5.38	3.38	0.298	0.25 3.25	3.00
6/01	7:40A 2:56P	64 78	14	Sunny Sunny	67 116	62 100	62 78	63.4 101.4	38.0	1.88 8.25	6.38	0.563	0.50 8.50	8.00
6/07	7:40A 3:02P	78 88	10	Ovrcest Sunny	82 118	78 110	78 89	79.1 109.3	30.2	2.38 7.75	5.38	0.474	0.50 7.50	7.00
6/12	7:44A 2:52P	81 92	11	Sunny Sunny	86 114	80 110	80 92	81.7 108.6	26.9	2.38 7.63	5.25	0.463	0.50 7.75	7.25
6/15	9:05A 3:24P	79 88	9	— —	90 118	82 110	79 90	83.9 109.4	25.5	3.75 7.50	3.75	0.331	0.25 7.00	6.75
6/20	9:00A 3:30P	84 96	12	Sunny Hazy	104 114	92 108	88 96	94.7 108.0	13.3	3.50 6.75	3.25	0.287	0.50 4.75	4.25
6/27	9:30A 2:40P	81 89	8	Ovrcest Sunny	93 119	81 112	81 91	84.4 111.0	26.6	3.50 8.00	4.50	0.397	1.50 8.50	7.00
7/03	8:20A 3:50P	79 91	12	Sunny Ovrcest	91 111	85 105	79 91	85.9 104.7	18.8	3.00 6.75	3.75	0.331	1.00 6.00	5.00
7/06	8:20A 3:00P	77 90	13	Sunny Ovrcest	87 100	77 90	77 85	79.9 92.1	12.2	3.13 5.50	2.38	0.210	0.50 4.00	3.50
7/11	8:30A 3:20P	82 91	9	Sunny Sunny	91 130	85 115	82 100	86.3 117.1	30.8	2.88 7.75	4.88	0.430	0.50 7.75	7.25
7/25	10:10A 3:20P	81 90	9	Sunny Ovrcest	108 121	92 110	90 97	96.3 111.3	15.0	4.75 8.00	3.25	0.287	2.25 7.75	5.50
8/03	9:10A 4:00P	72 80	8	Ovrcest Rainy	81 85	80 88	75 80	79.6 85.7	6.1	3.00 4.50	1.50	0.132	1.00 3.25	2.25
9/28	8:36A 3:00P	68 80	12	Sunny Ovrcest	70 90	68 88	68 78	68.6 87.2	18.6	2.63 6.00	3.38	0.298	0.25 4.00	3.75
10/02	9:05A 3:00P	54 75	21	Sunny Sunny	58 96	54 84	54 68	55.1 89.2	27.1	3.00 7.75	4.75	0.419	0.25 6.75	6.50
10/19	9:45A 3:50P	72 84	12	Ovrcest Ovrcest	80 94	76 84	76 80	77.1 86.3	9.2	2.75 4.75	2.00	0.176	0.50 3.75	3.25
11/02	8:23A 2:45P	60 56	4	Rainy Rainy	60 56	60 56	60 56	60.0 58.4	-1.6	2.38 2.38	0.00	0.00	0.75 0.75	0.00

*Col. (13) = Col. (12) ÷ 11.33

Sun Camber

continued

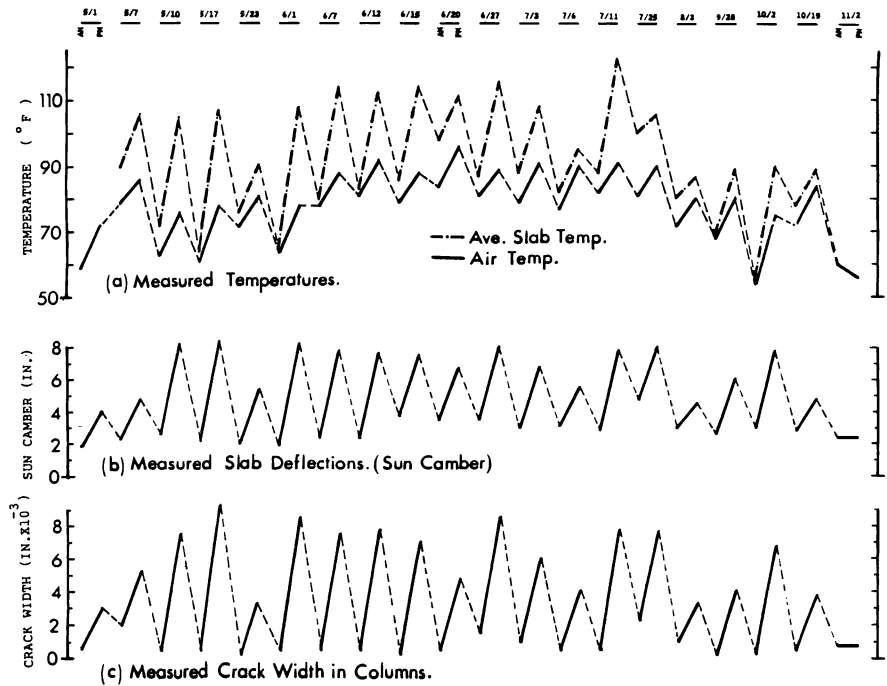


Fig. 8 — Plots of measured temperatures, sun camber, and crack widths.

- Deflections of the 60 ft (18.3 m) slab spans using the device shown in Fig. 7, which magnified slab deflections by 11.33.
- Crack widths in the exterior columns under the slab using an optical instrument with a magnification ratio of 50.
- Ambient temperatures and the corresponding weather conditions.

The above measurements were made each time in the morning (around 9:00 A.M.), and in the mid-afternoon (between 3:00 and 4:00 P.M.).

Table 1 is a summary of the recorded data. Fig. 8 shows plots of the 20 diurnal recordings of air temperatures, sun camber, crack widths in columns, and the computed average temperatures of the slab.

Temperature gradient and average slab temperature

Having measured the temperatures of the top of slab, bottom of slab, and bottom of beam, an average temperature through the slab section can be established. Considering the thermal properties of concrete and the time it takes for exterior (ambient) temperature changes to penetrate in the interior of concrete, it seemed appropriate, based on previous studies,¹ to use an equivalent steady-state linear gradient through the 4 in. (102 mm) slab and a parabolic gradient from the underside of the slab to the bottom of the beam (Fig. 6). The weighted (by cross-sectional area) average temperature t_{ave} for the entire section was then computed for each of the 17 data sets (the incomplete measurements from May 4, 7 and 10 were not included).

Considering the measured temperatures of the slab and the beam with their respective areas, a weighted t_{ave} is:

$$t_{ave} = \frac{\frac{t_{ts} + t_{bs}}{2} \times A_1 + \left(\frac{t_{bs} + t_{bb}}{2} + \frac{t_{bs} - t_{bb}}{6} \right) \times A_2}{A_1 + A_2}$$

Where A_1 = area of the slab (flange) cross-section
 A_2 = area of the beam (web) cross-section
 t_{ts} = temperature at top of slab
 t_{bs} = temperature at bottom of slab
 t_{bb} = temperature at bottom of beam

Column 9 of Table 1 shows the computed average temperatures across the slab section (including beam); column 10 shows the difference between the respective morning and afternoon slab temperatures; column 13 shows the corresponding differentials in slab levels. The average slab temperature change (morning to afternoon) to slab level change relationship is graphically presented in Fig. 10. A regression analysis of the 17 sets of data showed a correlation coefficient of 0.974.

Discussion of results of observations and measurements

The plot in Fig. 8a of the ambient temperatures and average slab temperatures shows very definitely the effect of direct solar radiation. In all twenty cases (except for the rainy day of November 2) the slab temperatures were to various degrees higher than the ambient temperatures. For example, on the clear sunny day of July 11, the top of the slab reached 130 F (54.4 C), was 39 F (21.7 C) hotter than the ambient temperature of 91 F (32.8 C) and was hotter than the bottom of the slab by 15 F (8.3 C). On this afternoon, the average slab temperature rose by 30.8 F (17.1 C) over that at 8:30 A.M., causing an increase in the sun camber of 0.43 in. (10.9 mm). During the same time the ambient temperatures rose by only 9 F (5 C).

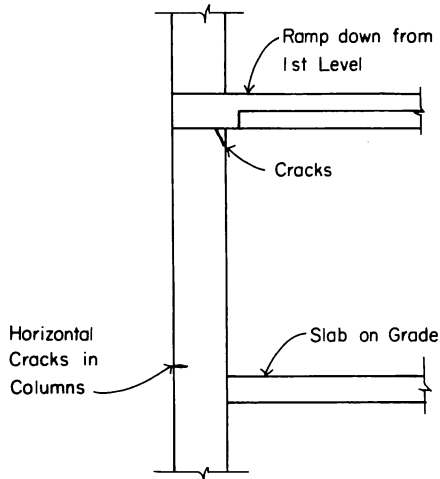


Fig. 9 — Section at ground level.

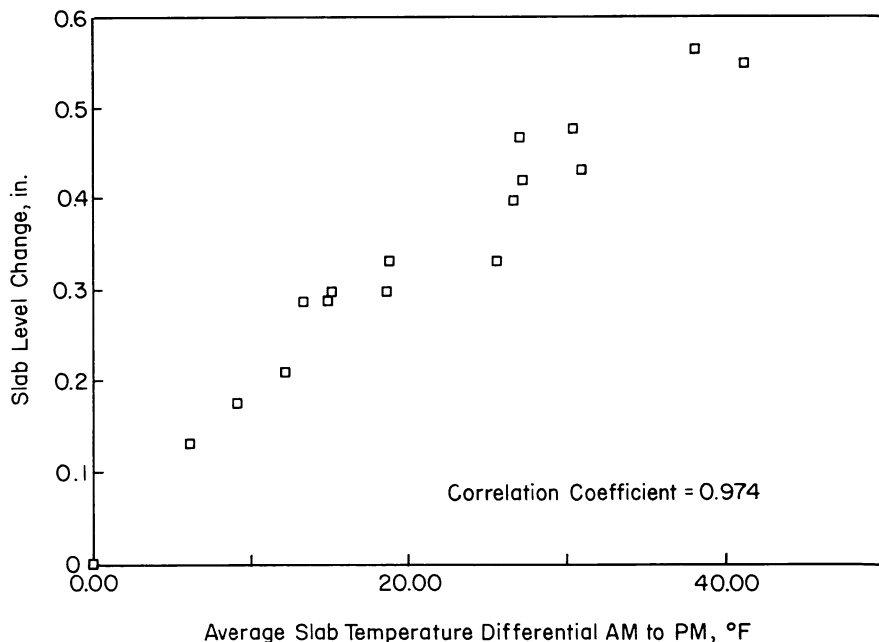


Fig. 10 — Plot of average slab temperature change vs. slab level change.

It is evident from the plot that the differentials of the slab temperature rose less on cloudy days. At the other extreme, the average slab temperature increased by only 6 F (3.3 C) on the rainy afternoon of August 3 (relative to the morning) while the air temperature increased by 8 F (4.4 C) during the same period. Also, the top of the slab was cooler than the bottom by 3 F (1.7 C) (this could be attributed to evaporative cooling).

The plot in Fig. 10b shows the measured differential upward slab deflections (sun camber) between the mornings and afternoons. The measurements were taken using the device shown in Fig. 7. A shortcoming of this measuring arrangement might be that the slab below the one whose deflections were being measured could also be undergoing some thermal deflections.

In Fig. 10c, crack widths in columns measured at locations shown in Fig. 5 are plotted. The crack widths are averages of measurements made on Columns G6, J6, P6 and R1.

Inspecting the plots in Figs. 8a, b, and c, for average slab temperatures, the sun camber, and crack width, respectively, it is evident that they are almost identical in their shapes. This indicates that, over the observed temperature range, the sun camber of the slab and the rotation of the spandrel beams were directly proportional to the factor causing them: a temperature gradient through the slab and beam. The results also lend confidence to the accuracy of the performed measurements.

Exterior beams of ramp down from first level

Several of the exterior beams of the ramp down from the first level (above the north-west entrance) had diagonal cracks at their soffits, some of them continued through the columns, causing tearing of the column corners under the beams. There were also horizontal

cracks on the outside faces of some of the columns above the slab on grade (Fig. 9).

The beam and column junctions had been repaired in recent years. Most repairs had subsequently failed. Examination indicated tensile forces directed inward and upward, supposedly caused by differential movements between the ground floor level and the first framed floor, due to:

- Continuous shortening of the slab system caused by creep due to post-tensioning and by slab shrinkage.
- Temperature contractions of the entire garage during the winter.

It could be further assumed that creep and shrinkage movements were at a very low rate 9 years after construction. The temperature contraction during the winter is a cyclic occurrence and must be structurally accommodated if the associated stresses cause cracking in already highly stressed members that have had their capacities reduced by years of subjection to tensile stress.

To verify these presumed reasons, several of the previous repair patches were removed and replaced with plaster of paris patches, so that occurrence of subsequent cracks and their widths could be observed both on a seasonal basis and during hot summer days.

Patches on distressed areas placed in May of 1984 had shown almost no signs of movement by November 1984. This indicated that the primary cause for the distress at this level was the winter shortening in the E-W direction of the entire 180-ft (54.9-m) wide garage relative to the ground.

Recommended repairs

The measured upward deflections during the six month period from May to November 1984, and their correlation with the air and roof slab temperature fluctuations, confirmed the initial assumption that sun camber caused by direct solar radiation was the primary cause of distress in the supporting beams. The

Camber Computations

The computed properties of a basic unit of floor (roof) system (Fig. A.1) are:

Cross-sectional area,

$$A = 433.3 \text{ in.}^2 (0.28 \text{ m}^2)$$

Distance of centroid from top of slab,

$$\bar{y} = 7.1 \text{ in. (180.3 mm)}$$

Moment of inertia of gross section about centroidal axis

$$I_g = 20,677 \text{ in.}^4 (0.0086 \text{ m}^4)$$

For the temperature gradient measured on the morning of June 1, 1984, assumed linear as shown in Figs. 6 and A.2, considering full restraint at the supports, the stress along the top surface

$$\begin{aligned} f_{rest} &= \alpha \Delta T E_c \\ &= -6 \times 10^{-6} (5) (4000) \\ &= -0.12 \text{ ksi (0.83 MPa)} \end{aligned}$$

where:

α is the coefficient of thermal expansion
 ΔT is the change in temperature
 E_c is the modulus of elasticity of concrete

The corresponding restraint force across the entire flange,

$$\begin{aligned} P_{rest} &= \frac{1}{2} f_{rest} h_f b \\ &= -\frac{1}{2} (0.12) (4) (60) \\ &= -14.4 \text{ kips (64 kN)} \end{aligned}$$

where h_f is the flange thickness and d is the flange width.

To release the restraint at the supports, axial forces equal and opposite to P_{rest} are applied at the ends of the roof unit along the line of action of P_{rest} (1.33 in. or 34 mm below the top surface of flange). This is equivalent to applying 14.4 kips (64 kN) of tension at the ends, acting along the centroidal axis of the roof unit, plus end moments equal to (Fig. A.4):

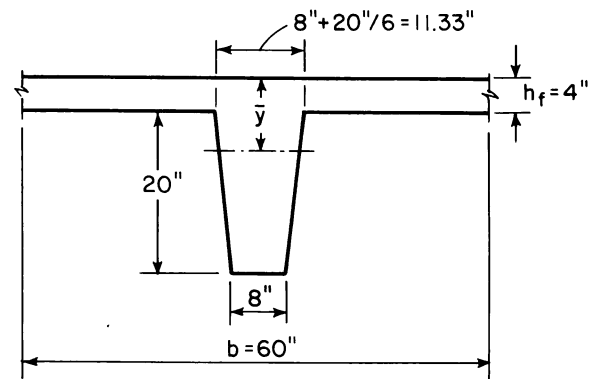


Fig. A.1 — Basic floor/roof system unit.

$$\begin{aligned} P_{rest} (\bar{y} - 1.33) &= 14.4 (7.1 - 1.33) \\ &= 83.1 \text{ in.-kips (9.4 kN-m)} \end{aligned}$$

The above bending moments acting at the ends would cause upward deflection of roof unit

$$\begin{aligned} \Delta_{midspan} &= \frac{M \ell^2}{8EI} \\ &= \frac{83.1 (720)^2}{8 (4000) (20677)} \\ &= 0.065 \text{ in.} \end{aligned}$$

For the temperature gradient measured on the afternoon of June 1, 1984, assumed linear-parabolic as shown in Figs. 6 and A.3, considering full restraint at the supports, the stress along the top surface

$$\begin{aligned} f_{rest} &= \alpha \Delta T E_c \\ &= 6 \times -10^6 (38) (4000) \\ &= -0.918 \text{ ksi (6.29 MPa)} \end{aligned}$$

The stress along the web-flange interface

good correlation between the computed sun camber and the field measurements reinforced this opinion.

During the nine year period since its construction, the structure had responded to these periodic movements by creating hinges at locations of maximum stress, thus relieving stress concentrations. Any repairs that did not consider these continual movements could not be successful.

To allow the structure to continue responding to external temperature effects without additional distress, it was judged prudent either to entirely relieve restraints to movement, or to accept the articulation locations created by the structure itself.

A desirable retrofit to remove the restraints on the roof against thermal movements is shown on Fig. 11. The detail shown, if provided on column lines 3 and 4

in bays F through S, would eliminate the slab restraints by cutting the slabs loose from the columns. The vertical column reinforcement would also be cut. The cutting operation would have to be carefully planned and executed to avoid injury to personnel, and to the structure, due to the possibility of explosive release of energy.

This detail would relieve the horizontal shear stresses in the inclined beams and allow future rotation of these beams together with the slab in response to sun camber. The existing cracks could be injected with epoxy to restore their original strength and then patched on the surface with cement grout to restore their appearance.

This very effective repair detail could not be implemented, as it was verified with the original construction company that there was no vertical cold joint be-

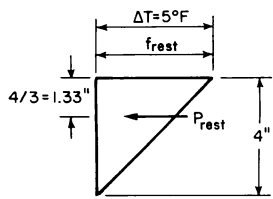


Fig. A.2 — Linear temperature gradient.

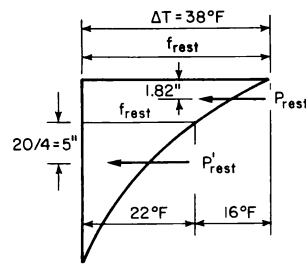


Fig. A.3 — Linear-parabolic temperature gradient.

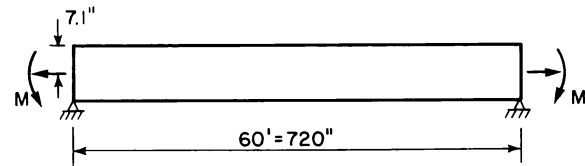


Fig. A.4 — Restraint-release forces and moments.

$$f'_{rest} = 6 \times 10^{-6} (22) (4000) \\ = -0.528 \text{ ksi (3.64 MPa)}$$

The corresponding restraint force across the flange

$$p_{rest} = \frac{f_{rest} + f'_{rest}}{2} h_j b \\ = \frac{0.912 + 0.528}{2} \times 60 \times 4 \\ = 172.8 \text{ kips (768.6 kN)}$$

Acting at a distance below the top surface which is equal to

$$\frac{22 \times 4 \times 2 + \frac{1}{2} \times 16 \times \frac{1}{3}}{11 \times 4 + \frac{1}{2} \times 26 \times 4} = \frac{176 + 42.67}{88 + 32} \\ = 1.82 \text{ in. (436.2 mm)}$$

The restraint force across the web

$$p'_{rest} = \frac{1}{3} f'_{rest} \times \text{web area} \\ = \frac{1}{3} (0.528) (193.3) \\ = 34 \text{ kips (151.3 kN)}$$

acting at an approximate distance below the flange-web interface

$$\frac{1}{4} \times 20 = 5 \text{ in. (127 mm)}$$

To release the restraint at the supports, axial forces equal and opposite to P_{rest} and P'_{rest} are applied at the ends of the roof unit along their respective lines of action. This is equivalent to applying 172.8 plus 34 kips (668.6 plus 151.3 kN) of tension at the ends, acting along the centroidal axis of the roof unit, plus end moments equal to

$$p_{rest} (\bar{y} - 1.82) + p'_{rest} (\bar{y} - 9) \\ = 172.8 (7.1 - 1.82) + 34 (7.1 - 9) \\ = 912.38 - 64.6 \\ = 847.8 \text{ in.-kips (95.8 kN-m)}$$

The corresponding

$$\Delta_{midspan} = \frac{M\ell^2}{8EI} \\ = \frac{847.8 (720)^2}{8 (4000) (20677)} \\ = 0.664 \text{ in. (16.9 mm)}$$

The difference in midspan deflections from morning to afternoon = $0.664 - 0.065 = 0.599$ in. (15.2 mm). This is very comparable to the measured value of 0.563 in. (14.3 mm).

tween the columns and beams as assumed in Fig. 11.

The subsequently recommended repair detail, which was implemented, is shown in Fig. 12. Since it had been determined that structural integrity was not affected by the presence of hinges, the primary objective of the repairs was to eliminate unsightly cracking and the misleading visual impression of structural deterioration.

The recommended detail had to be applied at all cracks in the supporting beams. It followed the structure's own selected articulation planes and allowed the beams to continue rotating the same way as they had done for years. The detail was designed to eliminate the unacceptable-looking jagged cracks and protect the reinforcing steel against corrosion. The neatly sawn joints were made between 1 and 2 in. (25 and 51 mm) wide, depending on the specific shape of each crack.

The major objective of this repair was to retain the status quo of the structure and to create esthetic-looking joints filled with a caulking compound. A layer of separation material assured that the caulking would adhere only at the saw cut (side) surfaces of the joints, thus preventing excessive local stretching and possible failure of the caulking material. When patching columns under the distressed beams, a separation, about $\frac{1}{2}$ in. (12 mm) deep, was required between each patch and the nearest beam underside. High quality workmanship was imperative.

Conclusions

Severe diagonal cracking of support beams and horizontal cracking of support columns in a 9-story cast-in-

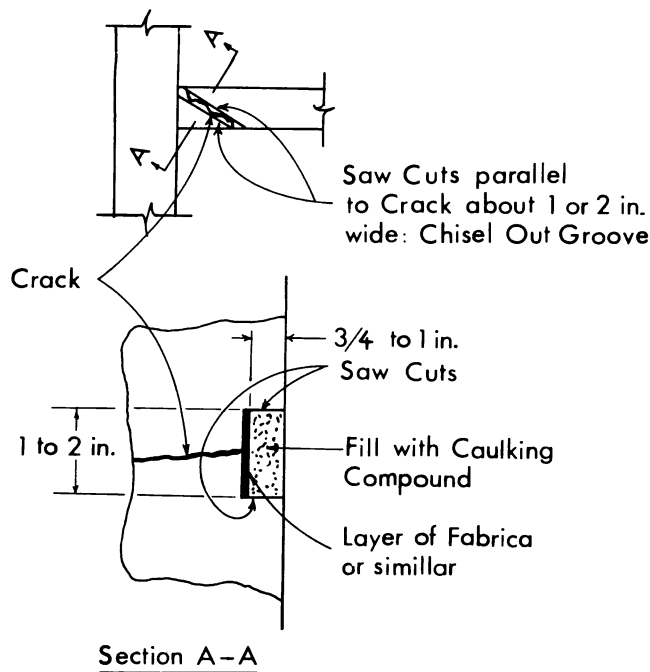


Fig. 11 — Detail for release of restraints.

place parking garage in Birmingham, Alabama was caused by vertical deflections of the 60-ft (18.3-m) span post-tensioned roof slabs. The following conclusions emerged:

- Field observations and measurements as well as analytical computations confirmed that large span roofs without insulation on the top are subject to significant vertical deflections (sun camber) as a result of temperature gradients through the exposed roof caused by direct solar radiation.
- On a sunny summer afternoon, the exposed top surface of the roof slab was 39 F (21.7 C) hotter than the ambient temperature and was hotter than the bottom of the slab by 15 F (8.3 C). This caused a sun camber of 0.43 in. (10.9 mm) on the 60 ft (18.3 m) span.
- Temperature increase at the top surface of the slab was significantly less on cloudy days.
- On a rainy afternoon the top of the slab was cooler than the bottom of the slab due to evaporative cooling.
- The superposition of torsional stresses over the heavy vertical and horizontal shear stresses in the beams supporting the 60-ft (18.3-m) span roof slabs caused cracking near the supports, creating hinges.
- Repeated patching of the cracks was unsuccessful, as the cracks continued to reappear.
- For repairs to be successful, movement of the roof should be made possible either by eliminating roof restraints, or by using repair details to allow the roof to articulate without causing cracking.
- The experience with this parking garage suggests that exposed roofs in multistory garages should preferably be simply supported, allowing both elongation and rotation at the supports, without causing over-stress. All other floors can be of continuous construction.

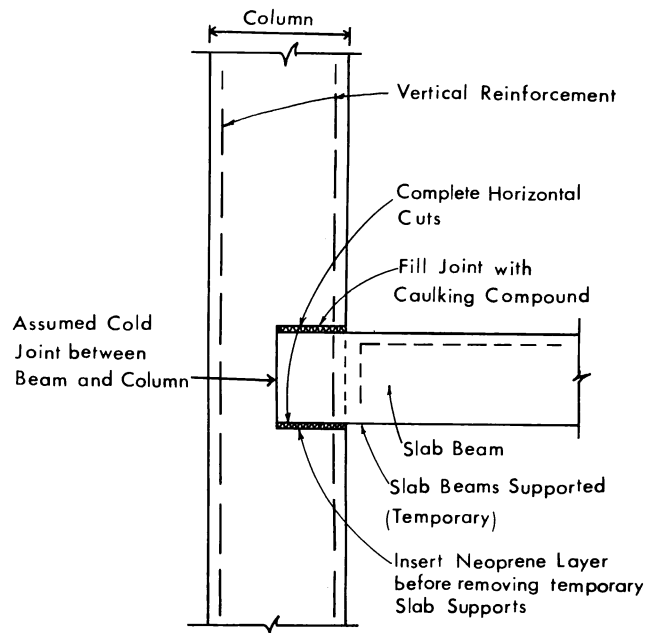


Fig. 12 — Detail for articulation joints in beams.

Acknowledgments

The authors wish to thank Ball, Marlin, Bridges & Associates of Birmingham, Ala., for their willingness to have this material published. Mohammad I. Kleit, teaching assistant in the Department of Civil Engineering, University of Illinois, Chicago, helped enormously with the preparation of the manuscript.

Reference

Fintel, M., and Khan, F.R., "Effects of Column Exposure in Tall Structures: Part A. Temperature Variations and Their Effects," *ACI JOURNAL, Proceedings* V. 62, No. 12, Dec. 1965, pp. 1533-1556.

Mark Fintel is a consulting structural engineer based in Chicago, Ill. He is a recognized authority on tall concrete structures and seismic design of concrete buildings. Prior to starting his consulting practice, he was director, advanced engineering services, Portland Cement Association, Skokie, Ill. He is the author of numerous publications, is a member of ACI-ASCE Committee 442, Response to Lateral Forces. He received the Wason Medal in 1971 and the Alfred E. Lindau Award in 1978.



ACI member **Satyendra K. Ghosh** is program manager, engineered structures, Portland Cement Association, Skokie, Ill. He served previously as associate professor of civil engineering at the University of Illinois at Chicago, and as principal structural engineer, advanced engineering services, Portland Cement Association. He has contributed to significant developments in the field of high-rise concrete buildings, and has published extensively in that field. He is a member of ACI Committees 209, Creep and Shrinkage, and 435, Deflection of Structures, and ACI-ASCE Committee 442, Response to Lateral Forces.

